# Supporting Information (SI)

## Co-Immobilization of Enzyme Conjugates on Hierarchical Large-Pore Mesoporous Silica for Efficient Cascade Transformations

Georgia Mhanna, Muslim Dvoyashkin, David Poppitz, Roger Gläser*

Institute of Chemical Technology, Universität Leipzig, Linnéstr. 3, 04103 Leipzig, Germany

* corresponding author

Email: roger.glaeser@uni-leipzig.de

### 1. *Preparation of Alkytrimethylammonium Hydroxide Solutions*

Aqueous solutions of alkyltrimethylammonium hydroxides $C_nTAOH$ (0.08 M) were prepared by ion exchange of alkyltrimethylammonium bromides $C_nTABr$ solutions (0.08 M) on Ambersep® 900(OH form) ion exchange resin (Alfa Aesar). The alkyltrimethylammonium bromides were purchased from Sigma-Aldrich (C12,14,16 with ≥ 95 %, ≥ 98 %, %, ≥ 98 % purity, respectively) and TCI Europe (C10,18 both with ≥ 98 % purity). Docosyltrimethylammonium bromide ($C_{22}TABr$) is synthesized by the reaction of 25 mL 2 M Trimethylamine in terahydrofurane (TCI Europe, 13 vol.-%) and 18.07 g 1-Bromodocosane (TCI Europe, > 98 %) in 100 mL butylacetate (Sigma Aldrich, > 99 %) in a stainless steel autoclave (V = 250 $cm^3$) at 399 K under autogeneous pressure for 24 h. The solid precipitate is filtered off, washed with butylacetate and used without further purification.

### 2. *Preparation of LPMS-x-yT Materials*

As shown in Fig. S1 (left), the DFT-method failed to describe the nitrogen sorption isotherm for large pore systems. Therefore, in the cases of partially transformed large-pore mesoporous silica materials, only the experimental points of the adsorption branch of the isotherm from the relative pressure P $P_0^{-1}$ between 0 and 0.95 were taken into account. Specific surface areas and specific pore volumes for both pore systems were determined by the t-plot method modified for LPMS-x and partial or fully transformed LPMS-x-yT-type silicas within the t-layer region from 0.6 to 1.3.[2] Fig. S1 (right) shows the fitting procedure for the material LPMS-50-33T. It can also be seen from the figure that from the conventional use of the t-plot in the layer region from 0.35 to 0.5, no microporosity appears in the samples.

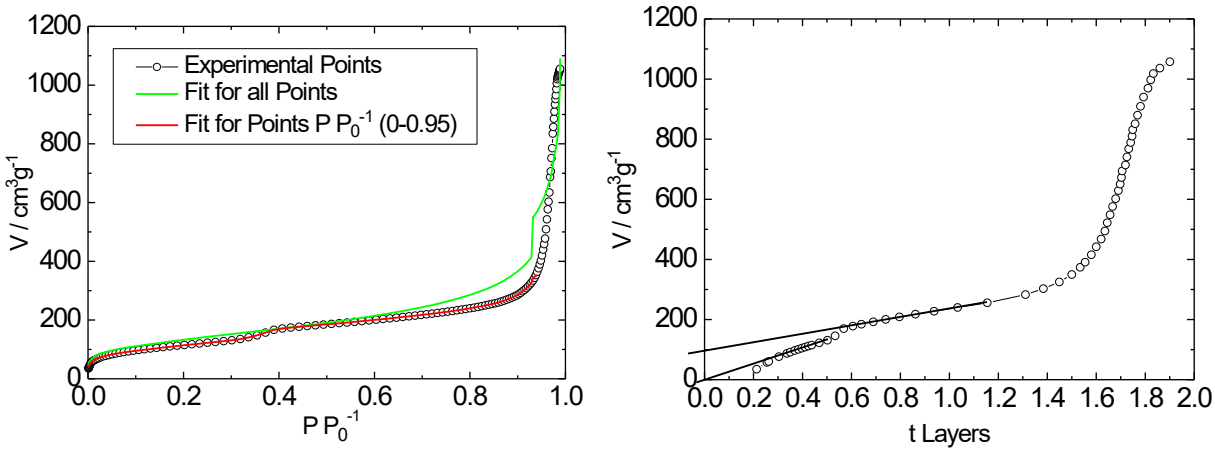


**Fig. S1:** Fitting procedures of the experimental points in the nitrogen adsorption isotherm (77 K) of LPMS-50-33T material by applying the DFT-method (left) and t-plot method (right).

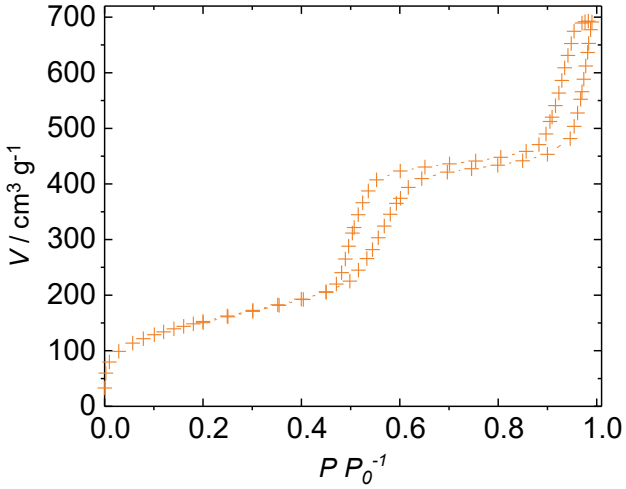


**Fig. S2:** Nitrogen sorption isotherms for the LPMS-material C22.

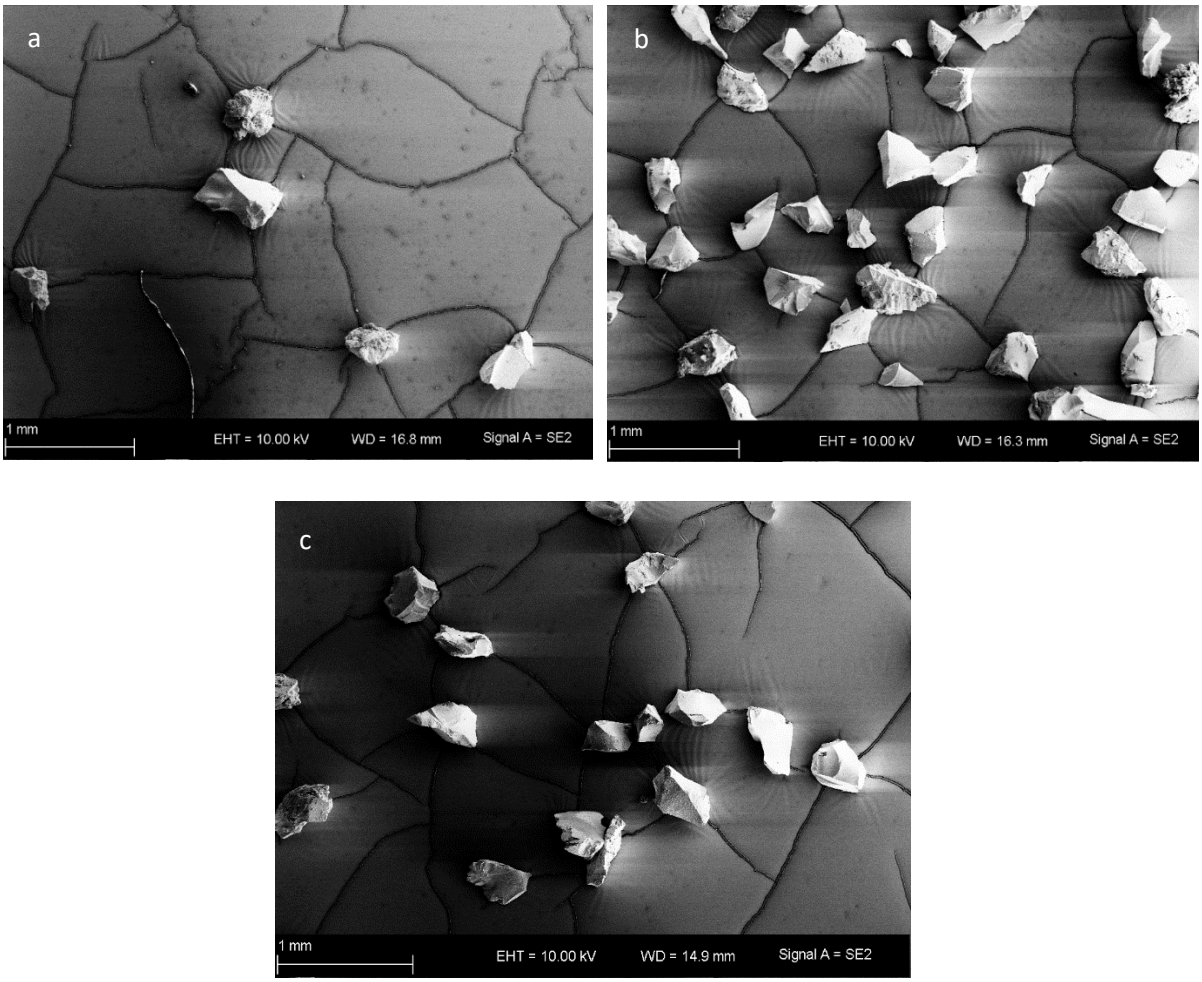


**Fig. S3:** SEM images of non-sieved LPMS (a), LPMS-50T (b), and LPMS-75T (c) materials showing no alteration of particle sizes and geometries before and after pseudomorphic transformation.

### *3. Preparation of Mesocellular Foam (MCF)*

The synthesis of a mesocellular foam (MCF) was based on a procedure reported by Han et al.[1]. 1.0 g Pluronic® P-123 (Sigma Aldrich) is dissolved in 16.3 mL deionized water and 2.5 mL hydrochloric acid (Sigma Aldrich, 37 wt.-%) at 313 K with stirring. After the addition of 2.0 g of 1,3,5-trimethylbenzene (TMB, Sigma Aldrich, 98 %), the mixture is stirred for 2 h at 313 K. 2.3 mL tetraethylorthosilicate (TEOS, Merck, 99 %) is slowly added dropwise to the emulsion and, after stirring for 5 minutes, the suspension is aged at 313 K for 24 h under static conditions. 11.5 mg of ammonium fluoride were added to the mixture which is stirred for one minute and then transferred to a 50 mL volume polytetrafluoroethylene (PTFE) bottle. After one day of aging at 363 K, the solid is filtered off, washed with deionized water (3 x 300 mL) and calcined at 813 K for 6 h in ambient air.

**Tab. S1:** Specific pore volume $V_P$, specific surface area $A_{(BET)}$, pore width $D_p$ and window size of synthesized MCF materials from nitrogen sorption at 77 K.

| Material | $V_P$ / $cm^3\ g^{-1}$ | $A_{(BET)}$ / $m^2\ g^{-1}$ | $D_p$ / nm | window size / nm |
|---|---|---|---|---|
| MCF | 2.84 | 588 | 22.1 | 17.6 |

## *4. Enzyme Immobilization*

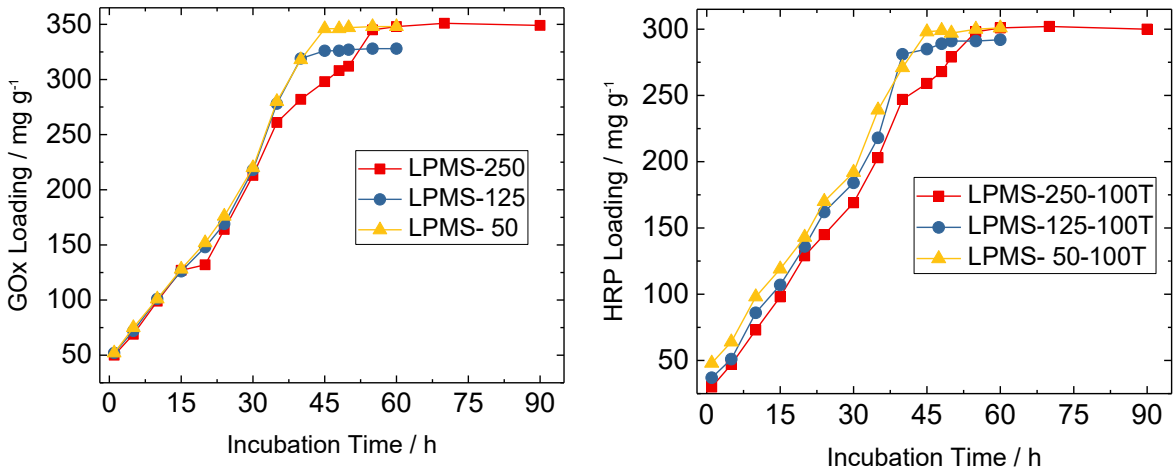


**Fig. S4:** Individual GOx loading (GOx solutions of 5 mg $mL^{-1}$, pH = 4.5) on large-pore mesoporous silica LPMS-x (left) and individual HRP loading (HRP solution of 5 mg $mL^{-1}$, pH = 5.0) on completely transformed large-pore mesoporous silica LPMS-x-100T as a function of incubation time. The loadings are shown for materials with different particle sizes, i.e., 50, 125 and 250 µm

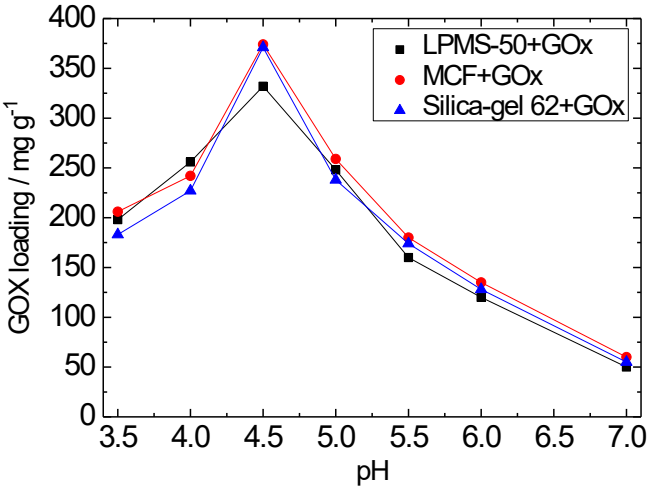


**Fig. S5:** GOx loading (GOx solutions of 5 mg mL-1) on large-pore mesoporous silica LPMS-50 and a mesocellular foam MCF and Silica-gel 62 as a function of the pH of the phosphate buffer solution.

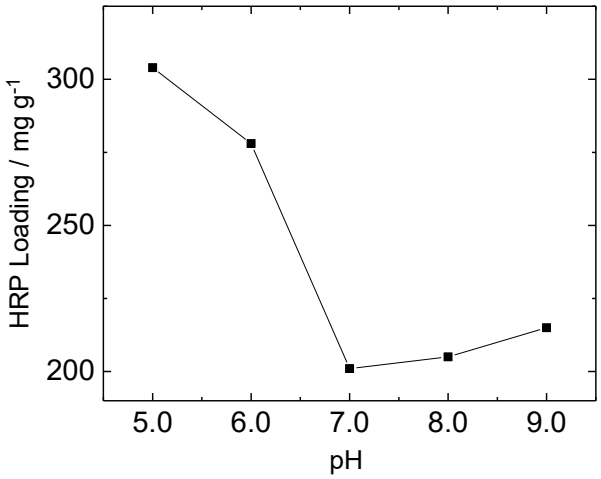


**Fig. S6:** HRP loading (HRP solutions of 5 mg mL-1) on completely transformed large-pore mesoporous silica LPMS-50-100T as a function of the pH of the phosphate buffer solution.

**Tab. S2:** Loading of GOx and HRP after sequential co-immobilization on the large-pore mesoporous silica with different maximum particle size and different MCM-41 pore fraction LPMS-x-yT.

| Support | HRP loading / mg $g^{-1}$ | GOx loading / mg $g^{-1}$ |
|---|---|---|
| LPMS- 50-50T+GOx/HRP | 128 | 350 |
| LPMS-125-50T+GOx/HRP | 125 | 347 |
| LPMS-250-50T+GOx/HRP | 129 | 328 |
| LPMS- 50-75T+GOx/HRP | 132 | 346 |
| LPMS-125-75T+GOx/HRP | 136 | 351 |
| LPMS-250-75T+GOx/HRP | 128 | 348 |

**Tab. S3:** Examples of calculation of loading of GOx and HRP after sequential co-immobilization on the large-pore mesoporous silica with different maximum particle size and different MCM-41 pore fraction LPMS-x-yT after subtracting the concentration of enzymes in the supernatant and washing solutions

| Support | initial mass of enzymes / mg | Total mass of enzymes in supernatant and washing solutions / mg | immobilized mass ($m_i$) / mg | (Enzyme loading)= $m_i/m_{silica}$ / mg $g^{-1}$ |
|---|---|---|---|---|
| LPMS-125-50T_Co-GOx HRP_pH 4.5 | 25 (GOx) | 9.92 | 15.08 | 301.68 (GOx) |
| LPMS-125-50T_Co-GOx HRP_pH 5 | 8.5 (HRP) | 3.29 | 5.21 | 104.30 (HRP) |
| LPMS-125-75T_Co-GOx HRP_pH 4.5 | 25.0 (GOx) | 9.86 | 15.14 | 302.79 (GOx) |
| LPMS-125-75T_Co-GOx HRP_pH 5 | 8.5 (HRP) | 3.31 | 5.19 | 103.70 (HRP) |

## 5. *Activity Studies and Enzymatic Kinetics*

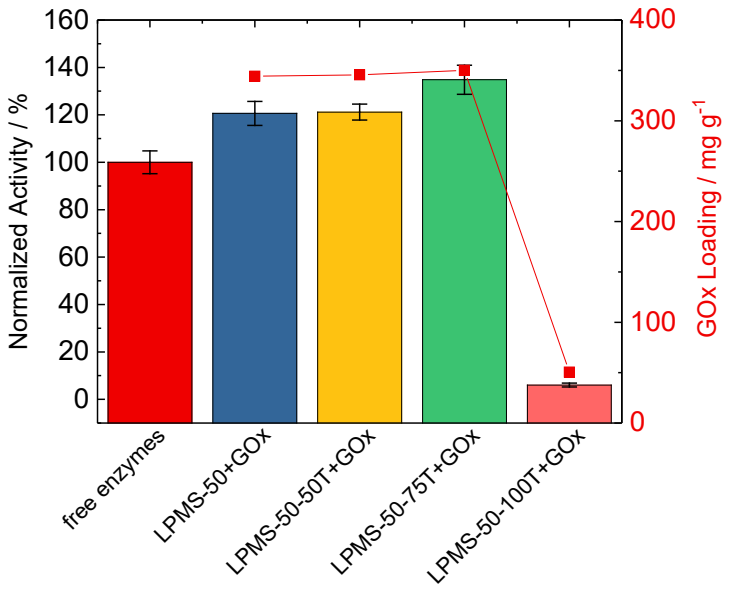


**Fig. S7:** Normalized activities of the free enzymes GOx and HRP and of GOx immobilized on large-pore mesoporous silica with different MCM-41 pore fraction LPMS-50-yT and free HRP. For the immobilized GOx also the GOx loadings are given.

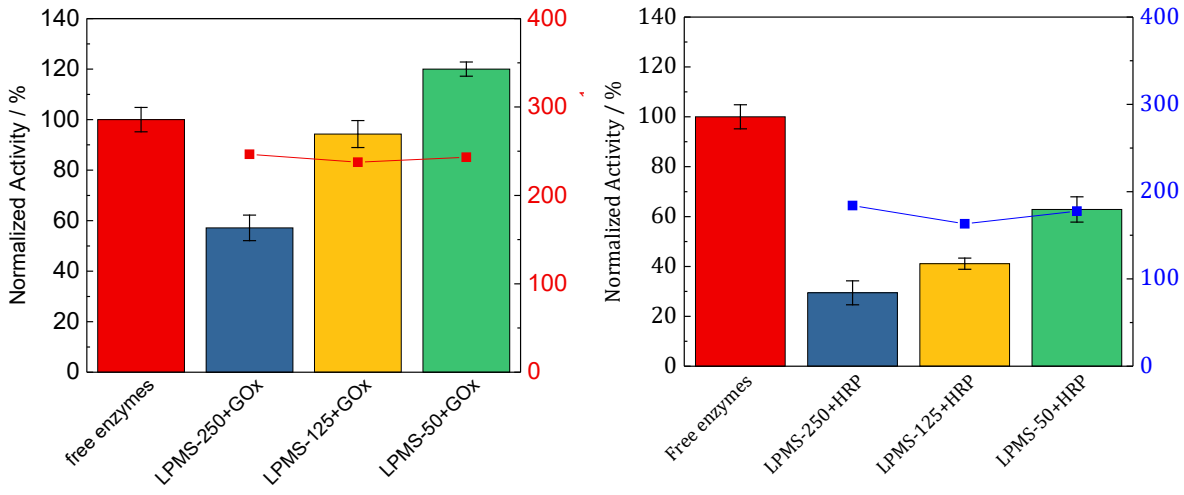


**Fig. S8:** Normalized activities of the free enzymes GOx and HRP and of GOx immobilized on large-pore mesoporous silica with different particle size LPMS-x and free HRP (left) and of the free HRP enzymes and of HRP immobilized on LPMS-x. For the immobilized enzymes, also the enzyme loadings are given.

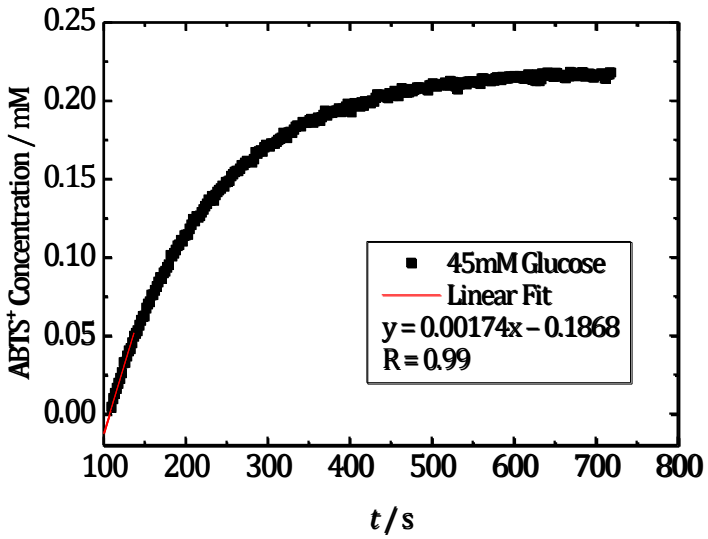


**Fig. S9:** Time dependence of $ABTS^{+}$ concentration with 45 mM glucose initial concentration for GOx individually immobilized on LPMS-50-50T (loading: 279 mg g-1) and HRP free. Initial reaction rate $r_0$ is determined by the linear fit as shown in the graph.

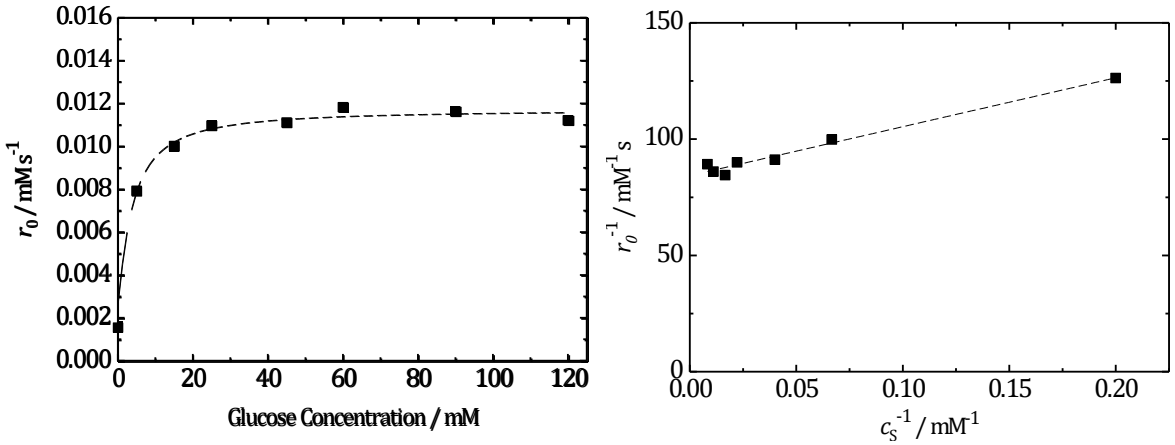


**Fig. S10:** Initial reaction rate ($r_0$) as a function of initial glucose concentration (left) and Lineweaver–Burk plot (right) for LPMS-50-50T+GOx catalyst and free HRP.

## 6. *Stability of the Immobilized Enzymes*

### 6.1. *Effect of Activity Assay Temperature*

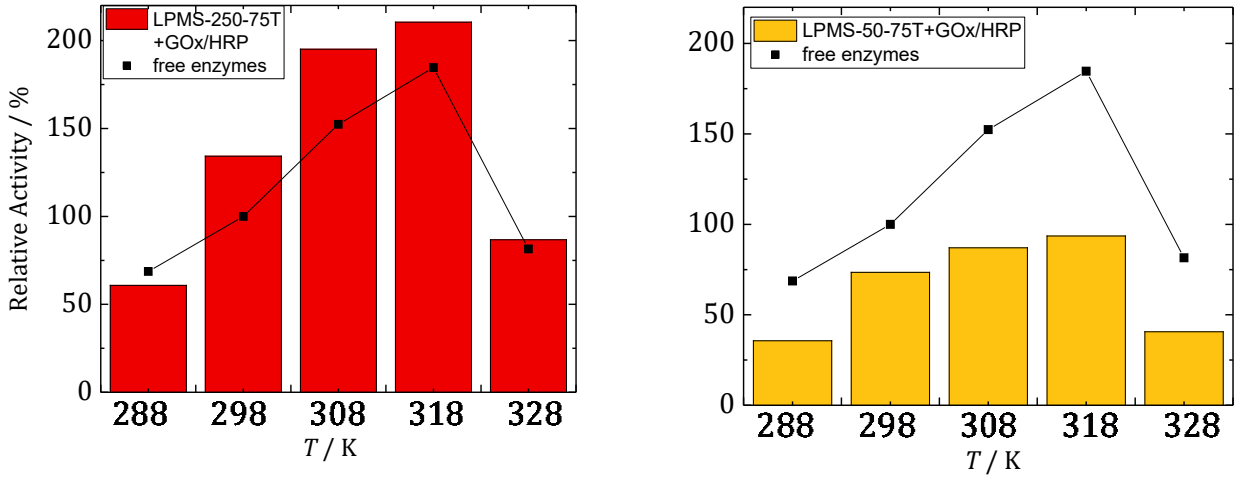


**Fig. S11:** Relative activity as a function of temperature of the medium during the activity assay for co-immobilized enzymes on hierarchical large-pore mesoporous silica LPMS-250-75T+GOx/HRP (left) and LPMS-50-75T+GOx/HRP catalysts (right) and for free enzymes GOx and HRP (black squares).

### 6.2. *Effect of Storage Temperature*

The activity of the HRP and GOx conjugate immobilized on LPMS-250-75T decreases by storage from 278 to 298 K, but maintains comparable to that of the free enzymes for up to an incubation temperature of 318 K for a duration of 4 h (Fig. S12). At 343 K and 353 K, the relative activities of the free enzymes drop to 30 % and 0 %, respectively, compared to the ones at 298 K. At these higher temperatures, the co-immobilized GOx and HRP are more active (55 and 35 % at 343 and 353 K,

respectively) than the free enzymes. This shows that the immobilization results in a higher stability towards temperature. This stabilizing effect is also observed when the two enzymes are supported on the LPMS-material with smaller particles size of max 125 µm LPMS-125-75T (Fig. S13),

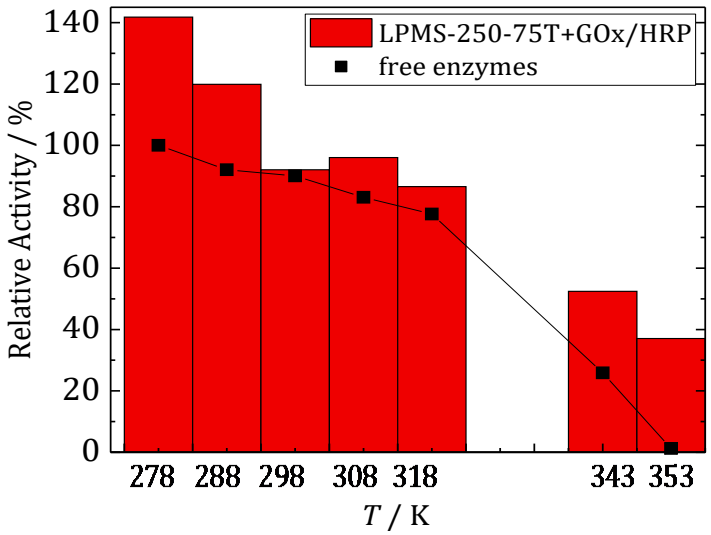


**Fig. S12:** Relative activity as a function of storage temperature for the co-immobilized enzymes GOx and HRP on hierarchical large-pore mesoporous silica LPMS-250-75T+GOx/HRP and for the free enzymes GOx and HRP (black squares).

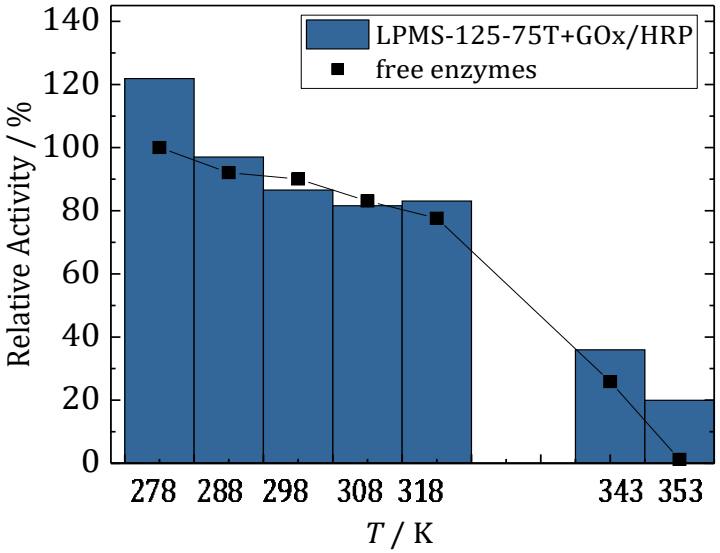


**Fig. S13:** Relative activity as a function of storage temperature for the co-immobilized enzymes GOx and HRP on hierarchical large-pore mesoporous silica LPMS-125-75T+GOx/HRP and for the free enzymes GOx and HRP (black squares).

When the particle size of the support is even smaller, i.e., 50 µm, the activity of the immobilized enzymes is lower than for the free enzymes already at the temperatures below 318 K, while similar activities are achieved at the higher temperature of 343 and

353 K (Fig. S14). This observation is in accordance with the previous conclusion that the enzymes supported on the smaller particles of LPMS-50-75T are located rather in the outer pores, i.e., closer to the outer surface.

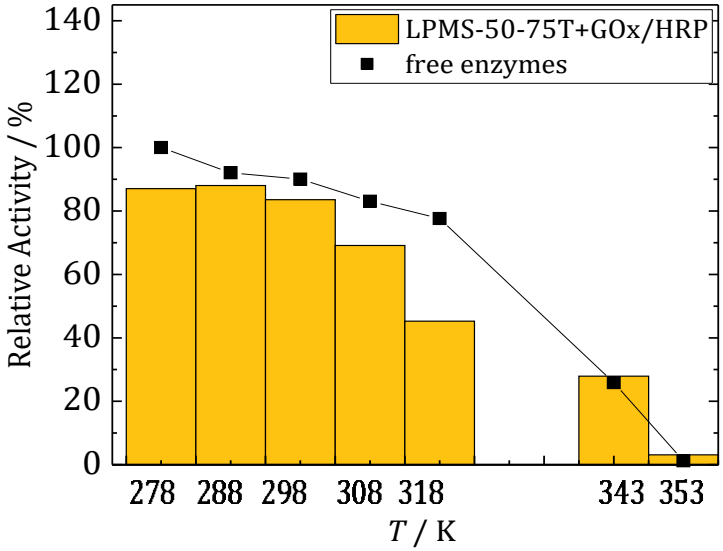


**Fig. S14:** Relative activity as a function of storage temperature for the co-immobilized enzymes GOx and HRP on hierarchical large-pore mesoporous silica LPMS-50-75T+GOx/HRP and for the free enzymes GOx and HRP (black squares).

### *6.3. Effect of Storage Time*

The stability of free GOX and HRP and of GOx and HRP immobilized on partially transformed LPMS-materials with different particle sizes LPMS-x-75T was studied for incubation times from 0 to 15 days at 278 K. The observed relative activities are referred to the activity of the fresh, non-stored free GOx and HRP in solution at 298 K as 100 %. As shown in Fig. S15, all biocatalysts become less active over storage time, most likely as a result of enzyme leaching. Note that the slope of the activity decrease with the duration of storage is similar for all catalysts studied. This points at the same cause of deactivation (denaturation) for all catalysts. Note also that the activity of the enzymes immobilized on the supports with 125 and 250 µm maximum particle size, i.e. LPMS-125-75T and LPMS-250-75T, remains higher than that of the free enzymes over whole period of investigated storage time. The activity for the hierarchical LPMS-material with 250 µm particle size decreases even less strongly from 9 days storage onwards. These high stability for supports with larger particles provides further support for the earlier conclusion that the enzymes in the larger particles are located within the pores of the monolithic particles and are, thus, more efficiently protected from leaching.

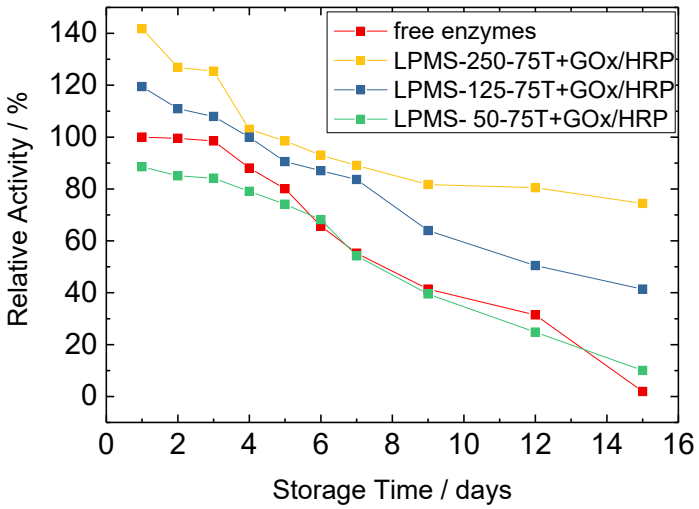


**Fig. S15:** Relative activity as a function of storage time for the co-immobilized enzymes GOx and HRP on hierarchical large-pore mesoporous silica LPMS-x-75T+GOx/HRP and for the free enzymes GOx and HRP (red squares) at 278 K.

# References

(1) Han, Y.; Lee, S. S.; Ying, J. Y. Pressure-driven enzyme entrapment in siliceous mesocellular foam. *Chem. Mater.* **2006**, *18*, 643–649.

(2) Galarneau, A.; Villemot, F.; Rodriguez, J.; Fajula, F.; Coasne, B. Validity of the t-plot method to assess microporosity in hierarchical micro/mesoporous materials. *Langmuir* **2014**, *30*, 13266–13274.